Отримано експериментальне підтвердження можливості вимірювання внутрішньої температури біологічного об'єкта по тепловому акустичному випромінюванню з точністю не нижче 0,2 °С в реальному масштабі часу акустотермометром, що реалізує модифікований нульовий модуляційний метод. Розроблено макетний зразок одноканального пасивного неінвазивного акустотермометра з фокусуванням на основі пластинчатого п’єзокерамічного електроакустичного перетворювача, акустичної еліптичної лінзи і блоків двох серійних вольтметрів. Запропонована електронна комутація вихідних сигналів імітатора шуму та еквівалентної схеми п'єзоперетворювача, при якій опір генерує тепловий шум з інтенсивністю, рівною сумі інтенсивностей акустичного випромінювання біологічного об'єкту та власного шуму п'єзоперетворювача. Таке схемотехнічне рішення дозволило виключити зі схеми акустотермометра блок механічного модулятора (обтюратора), який дотепер використовувався в аналогах. При розробці оригінального блоку комутації та детектування для модуляції вхідного шумового сигналу було запропоновано використовувати ключовий режим роботи польових транзисторів з вбудованим n-каналом. Проведено розрахунок еквівалентних схем п'єзоприймача та імітатора шуму, що являють собою зв’язані контури зі смугою пропускання, в якій середній рівень шумової напруги визначається напругою шуму на частоті електричного резонансу п'єзоелемента. Доведено можливість використання макету одноканального неінвазивного акустотермометра з фокусуванням, побудованого по схемі, що реалізує модифікований нульовий модуляційний метод, для вимірювання шумових напруг в діапазоні від 5 до 30 мкВ. Оскільки процес виготовлення або експлуатації п'єзоелектричного перетворювача може призвести до відхилення його параметрів від теоретично розрахованих, була розроблена методика, що дозволяє виміряти амплітудно-частотні характеристики активної та реактивної складових електричного імпедансу. Проведено контроль якості складання п'єзокерамічного електроакустичного перетворювача з фокусуванням і отримана залежність напруги електричних шумів на електродах п'єзоелектричного приймача з фокусуванням від температури

Ключові слова: ультразвук, акустотермометрія, внутрішня температура, п’єзоелектричний перетворювач, акустотермометр, теплове акустичне випромінювання

UDC 534.08

DOI: 10.15587/1729-4061.2020.192594

EXPERIMENTAL RESEARCHING OF BIOLOGICAL OBJECTS NONINVASIVE PASSIVE ACOUSTO-THERMOMETRY FEATURES

V. Didkovskyi
Doctor of Technical Sciences, Professor*
Email: vs.didkovskyi@aae.kpi.ua

S. Naida
Doctor of Technical Sciences, Professor*
E-mail: s.naida@kpi.ua

O. Drozdenko
PhD, Associate Professor*
Email: oi.drozdenko@gmail.com

K. Drozdenko
PhD*
Email: k.s.drozdenko@gmail.com

*Department of Acoustics and Acoustoelectronics
National Technical University of Ukraine "Igor Sikorsky Kyiv Polytechnic Institute"
Peremohy ave., 37, Kyiv, Ukraine, 03056

Received date 21.11.2019
Accepted date 20.01.2020
Published date 24.02.2020

1. Introduction

Today, a rather relevant direction in medicine is the study of passive functional images of biological objects, in particular, a human body, obtained by methods of recording physical fields of various nature, among which infrared (IR) thermal imaging, radio and acoustic thermometry can be distinguished.

IR thermal imaging is characterized by a penetration depth of about 100 μm and allows obtaining information about the surface temperature due to capillary blood flow in the skin. Radio and acoustic thermometry allow measuring the temperature of internal tissues at depths of several centimeters, which is of interest in early diagnosis of diseases, hearing diagnostics, identifying inflammatory processes, monitoring physiotherapy procedures, conducting surgical operations accompanied by patient cooling, long-term control of the engraftment process of transplanted organs, monitoring treatment of malignant neoplasms by hyperthermia and thermal ablation methods, as well as using synergistic effects in oncology.

In the acoustothermometry research method, the internal temperature is measured by receiving and recording acoustic radiation generated by the thermal motion of atoms and molecules of the medium. Thermal acoustic radiation is low-power noise radiation with a wide spectrum, and its intensity is directly proportional to thermodynamic temperature.

Comparative analysis of radio and acoustic thermometry [1] showed that the method of measuring the internal temperature by recording thermal acoustic radiation has a better spatial resolution, less attenuation and is also easier to implement, which proves the prospects of its use.

2. Literature review and problem statement

In [2], an acoustic thermometer (AT) was proposed to measure the internal temperature of a biological object, the operation of which is based on the zero modulation method. This method allows distinguishing weak noise signals, which include thermal acoustic radiation, against the background of the receiver's natural noise. Detailed analysis of the modulation AT based on the results of [3–6] showed that the minimum detected temperature difference is much worse than the maximum allowable one calculated theoretically. In addition to this drawback, such an AT has limited application due to the need for a priori knowledge of frequency-dependent absorption coefficients and measurements at two frequencies.

An option to overcome these difficulties may be the use of a focused piezoelectric receiver in the AT. In [1], based on the study of the features of receiving thermal acoustic radiation depending on the design of the piezoelectric receiver (PR), the principles of constructing the corresponding element of the receiving path were formulated.

The works [7, 8] were devoted to the search for circuitry solutions of the acoustic receiver and materials of its structural units, the implementation of which made it possible to obtain sufficient accuracy of internal temperature measurement for medical applications.

In [9], on the basis of the theory of human body acoustothermometry, a block diagram of the focused AT implementing the modified zero modulation method was theoretically justified and developed. It is shown that the use of a piezoelectric plate as a noise signal receiver, taking into account the effect of spatial filtering of diffuse radiation by transition layers, makes it possible to do with single-spectrum and single-beam sounding. The use of electronic switching of the piezoelectric transducer and the noise standard allowed excluding the modulator unit used in analogs from the acoustic thermometer circuit. From the results of theoretical studies, it was concluded that the proposed AT allows real-time temperature measurement by thermal acoustic radiation through the skin with an accuracy of at least 0.2 °C.

The practical significance of the results is obvious, but the issues regarding the experimental validation of the presented analytical calculations were not sufficiently addressed. AT functioning is associated with the measurement of weak noise signals in the megahertz range. In addition, during assembly and operation, deviations of parameters from those theoretically calculated may occur, so it is necessary to have information on the degree of accuracy with which the proposed mathematical models describe real physical phenomena.

The above suggests it advisable to conduct laboratory studies in this direction.

3. The aim and objectives of the study

The aim of this work is to verify the compliance of analytical calculations with practical implementation, as well as experimental confirmation of the possibility of measuring the deep temperature of the AT implementing the modified zero modulation method with a given accuracy.

To achieve the aim, the following objectives were set:

– to create a model of a single-channel focused AT;

– to conduct an experimental study of electric noise voltage at the electrodes of the focused piezoelectric receiver from temperature according to the established method.

4. Model of the single-channel focussed acoustic thermometer

The AT model (Fig. 1) contains an acoustic receiver (AR) connected to a broadband high-frequency amplifier (HFA), amplitude (AD) and synchronous (SD) detector, from the output of which the signal is transmitted to a recording device (RD).

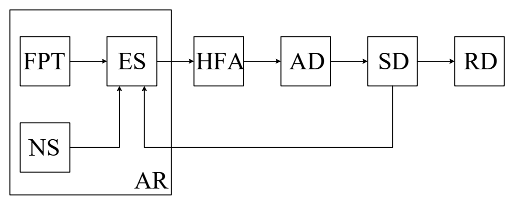

a

b

Fig. 1. Model of the focused AT: *a* — block diagram; *b* — appearance

The acoustic receiver includes a focussed piezoelectric transducer (FPT), an electronic switch (ES) and a noise simulator (NS). As the FPT of thermal acoustic radiation, a PZT-8 piezoceramic plate transducer with a quarter-wave matching layer of epoxy glue and an acoustic lens made of polystyrene mechanically non-damped from the back side and electrically loaded with parallel-connected inductance is used.

The noise simulator has the same frequency response as the focused piezoelectric transducer and close value of the mean square of the output voltage. The electronic switch periodically switches the input of the high-frequency amplifier from the focused piezoelectric transducer to the noise simulator and back.

The model includes the original switching and detection unit, as well as two serial devices – V3-57 microvoltmeter and V7-27 universal digital voltmeter. V3-57 is designed to measure the RMS value of arbitrary shape AC voltage, and V7-27 is used to measure DC and AC voltage, resistance, direct current, temperature by converting the measured physical value into DC voltage and then measuring it with an integrating analog-to-digital converter.

The V3-57 microvoltmeter used its broadband amplifier, and the V7-27 versatile digital voltmeter – constant voltage modulation unit; AC voltage amplifier; synchronous detector; low-pass filter; digital voltage meter proportional to the temperature difference between the biological object and noise simulator.

4. 1. Noise simulator of the focused piezoelectric transducer

As a noise simulator, it is proposed to use a resistor with a resistance *R*=7,700 Ohm and reactive elements forming a band-pass filter for the thermal noise of this resistor (Fig. 2) (nominal values of filter elements are equal to those of elements of the PR equivalent circuit).

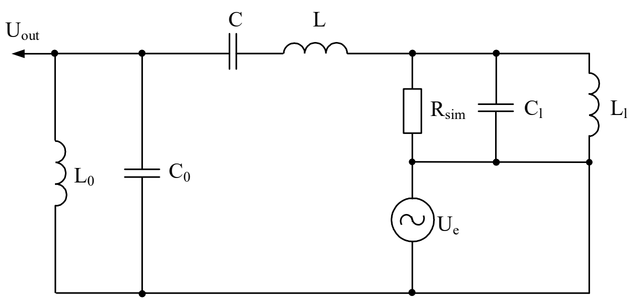

Fig. 2. Equivalent circuit of the electric noise simulator

Parameters of the elements of the band-pass filter of the electric NS for $k_t = 0.51$; $\beta = k_t^2 = 0.26$ (k_t – electromechanical coupling coefficient of piezoceramics) are determined as follows:

$$C_0 = 157 \text{ pF};$$

$$L_0 = 1/\omega_0^2 (C_0 + C_{cab});$$

$$C = C_0 (8\beta/\pi^2)/(1 - 8\beta/\pi^2); \quad L = 1/\omega_1^2 C,$$

where C_0 is the static capacitance of the piezoelectric element, C_{cab} is the capacity of the connecting cable, $\omega_1 = \omega_0 (1 - 8\beta/\pi^2)^{1/2}$ is the angular frequency of electric resonance of the piezoelectric element (resonance frequency), ω_0 is the angular frequency of mechanical resonance of the piezoelectric element (antiresonance frequency).

4. 2. Electronic switch of the focused electric converter and noise simulator

In classical modulation AT, modulation of the noise signal of a biological object is performed by a rotating disk with holes. In the case of a depth-focused piezoelectric receiver, such modulation is not possible, so it was proposed to use an electronic switch.

The key mode of semiconductor elements (diodes, transistors) is widely used in voltage switches. However, the case of thermal noise switching was not found in the literature. In this regard, the original switching and detection unit was developed (Fig. 3).

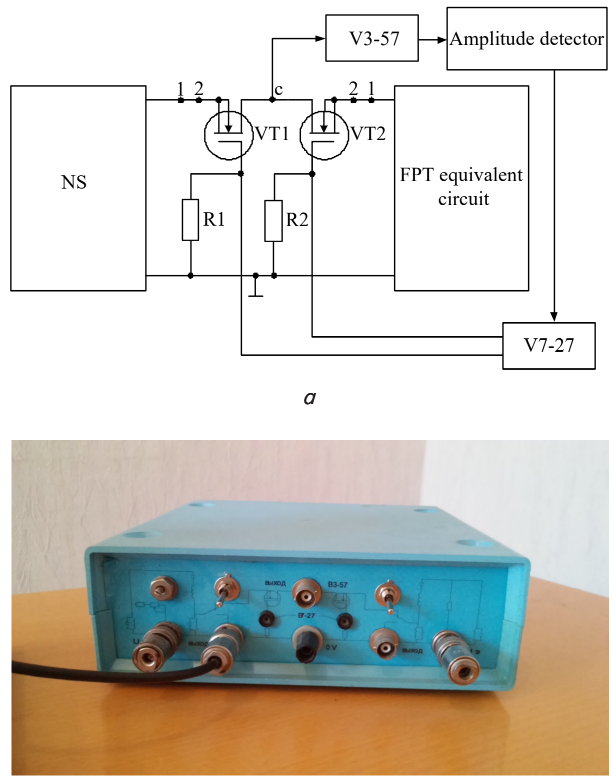

Fig. 3. Switching unit: *a* – electronic switch with noise simulator and FPT equivalent circuit in the block diagram of the AT model; *b* – appearance

The switch of the focused electric converter and noise simulator is made on n-channel field-effect transistors (FET). Transistors of this type at drain-source voltages of both signs less than 1 V are controlled resistors, the resistance of which is minimum at the gate-source voltage $U_{g\text{-}s} = 0$ and very large at $|U_{g\text{-}s}| > U_{cutoff}$ (U_{cutoff} – cutoff voltage). The channel of the field-effect transistor can be bulk (junction gate transistors) and surface (insulated gate transistors) [10, 11].

The resistance of the junction gate transistor is minimum when the gate-source voltage $U_{g\text{-}s} = 0$. Reference books usually give the value of the initial drain current I_{ind} at a saturation voltage $U_{d\text{-}g\ sat}$, and also the cutoff voltage $U_{g\text{-}s\ cutoff}$. Equality $U_{d\text{-}ssat} = U_{g\text{-}s} - U_{g\text{-}scutoff}$ or $U_{d\text{-}ssat} = -U_{g\text{-}scutoff}$ at $U_{g\text{-}s} = 0$ always holds.

Therefore, the value r_{d-s0} can be determined by the formula:

$$r_{d\text{-}s0} = \frac{U_{d\text{-}ssat}}{2I_{dsat}} = -\frac{U_{g\text{-}scutoff}}{2I_{ind}} > 0.$$

4. 3. Equivalent circuit of the focused piezoelectric receiver

The equivalent circuit of the piezoelectric receiver (Fig. 4), like the noise simulator, are connected circuits with a bandwidth in which the average noise voltage level is determined by the noise voltage at a frequency:

$$f_1 = \frac{1}{2\pi\sqrt{LC}} = f_0 \sqrt{1 - \frac{8k_t^2}{\pi^2}}. \quad (1)$$

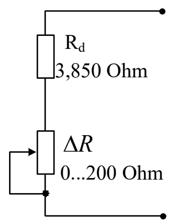

Fig. 4. Equivalent circuit of the piezoelectric transducer at resonance frequency

Assuming that in the range Δf the resistance $R = R_d + \Delta R$, we get:

$$\overline{U}_{\text{ш}}^2 = 5.52 \cdot 10^{-23} \left(R_d + \Delta R\right) T \Delta f_{\text{sim}}. \tag{2}$$

From (2), it follows that the resistance $r_{\text{d-s}}$ (for $U_{\text{g-s}} = 0$) should be much less than $R_d + \Delta R$.

5. Experimental study of the AT model

The experimental study of the model was carried out in several stages.

At the preparatory stage, according to the developed method, a set of measurements was carried out aimed at checking the compliance of the NS characteristics and the FPT equivalent circuit (Fig. 5), as well as voltage values at the control points of the model, with theoretically calculated.

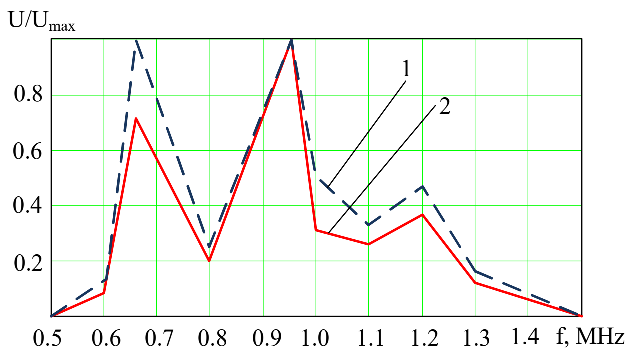

Fig. 5. Experimental normalized frequency response of the equivalent circuit of FPT (curve 1), NS (curve 2)

Noise voltage at a separate resistance with a nominal value of 3,850 Ohm (7,700 Ohm) at the input of the V3-57 microvoltmeter was estimated (Table 1). Instead of the FPT, its equivalent circuit was used, similar to that of the noise simulator, in which resistance generates thermal noise with an intensity equal to the sum of intensities of the received acoustic radiation of the biological object and natural noise of the piezoelectric transducer.

Since the V3-57 bandwidth is [5 Hz...5 MHz], that is, 10 times greater than Δf=0.5 MHz, the noise voltage should be about 114 μV. The results in Table 1 show that the theoretical and experimental values are almost identical.Subsequent studies focused on measuring the frequency dependences of the FPT electrical impedance in order to determine the nature of changes in the electric voltage at the electrodes of the transducer under test to control the assembly quality. The measurements were carried out according to the block diagram implemented in the experimental stand (Fig. 6).

Table 1

Measured noise voltage at a separate resistance at the V3-57 microvoltmeter input

Rated resistance	Noise voltage
3.3 kOhm	60 μV
7.5 kOhm	100 μV

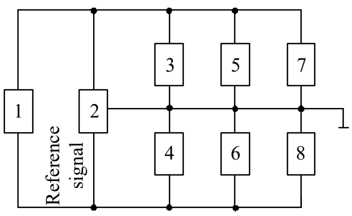

Fig. 6. Block diagram of the experimental stand for measuring frequency dependencies of FPT electrical impedance

According to standard methods [10, 11], the voltage from generator 1 with a given frequency and amplitude U_1, maintained constant (controlled by voltmeter 5), was supplied through ballast resistor 7 to piezoelectric element 8.

Voltmeter 6 measured the voltage amplitude at the piezoelectric element U_2, and phase meter 2 measured the phase angle φ_1 between the voltages U_1 and U_2. Frequency meter 3 and oscilloscope 4 controlled the output signal by frequency and appearance. In this case, resonance and antiresonance sections of frequency response were detected.

The dynamic range and levels of the signals used U_1 were determined in accordance with the resulting interference level U_n. In this case, the ratio $U_1 / U_n \geq 20\,\text{dB}$ holds as follows:

– in the absence of voltage at the output of generator 1, the interference voltage U_n; at the test object 8 was measured;

– electric voltage exceeding the interference voltage by at least 20 dB was set on the test model 8.

The values of impedance, as well as its active and reactive components, were determined by the formulas:

$$z = \frac{U_2}{U_1} R_0;$$

$$R_a = R_0 \frac{U_1}{U_2} \frac{\cos\varphi - U_1/U_2}{\sin^2\varphi + \left(\cos\varphi - U_1/U_2\right)^2};$$

$$X_e = R_0 \frac{U_2}{U_1} \frac{\sin\varphi}{\sin^2\varphi + \left(\cos\varphi - U_2/U_1\right)^2}, \tag{3}$$

where the cosine of the phase difference between current and voltage was determined by the formula: $\cos\varphi = \cos\left(180° - \varphi_1\right)$, where φ is the phase difference between current and voltage.

The experimental frequency response of the focused AT piezoelectric transducer, in accordance with (3), is presented in Fig. 7.

To analyze the obtained frequency response, a method based on the use of equivalent electrical circuits was applied (Fig. 8) [12, 13].

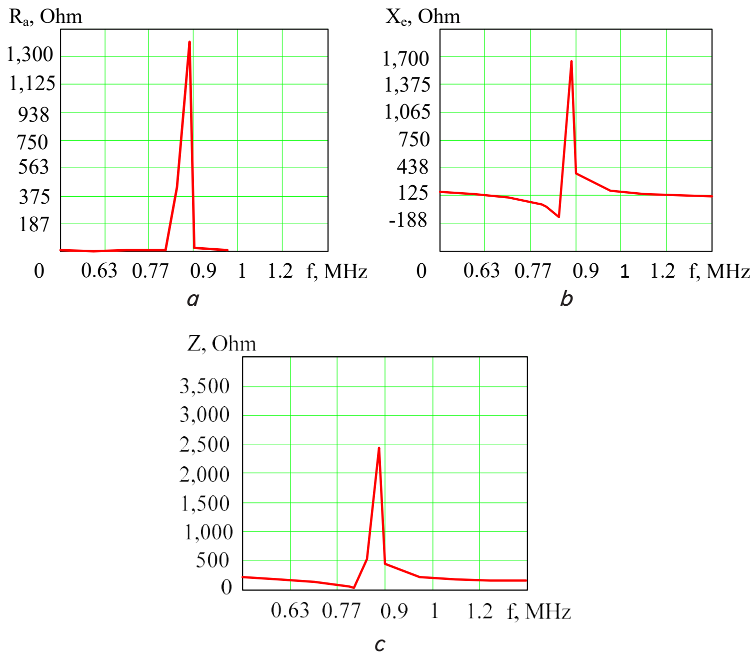

Fig. 7. Experimental frequency response: *a* – active; *b* – reactive component of electrical impedance of the piezoelectric receiver; *c* – electrical impedance of the piezoelectric receiver of the acoustic thermometer

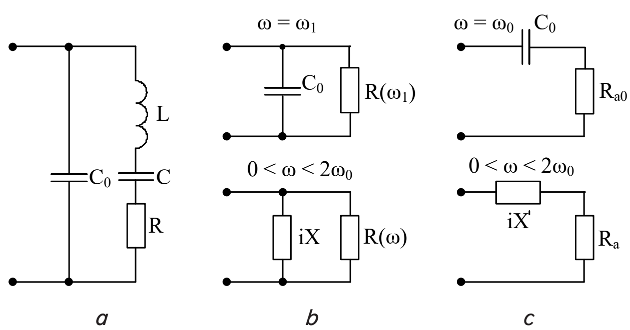

Fig. 8. Transducer equivalent circuits: *a* – general case; *b* – parallel equivalent circuit; *c* – serial equivalent circuit

On equivalent circuits (Fig. 8), the following notation is used:

$$C=\frac{8C_0k_t^2/\pi^2}{1-8k_t^2/\pi^2}\approx\frac{8C_0k_t^2}{\pi^2}$$

– dynamic capacitance; C_0 – static capacitance of the piezoelectric element;

$$L=\frac{1}{C\omega_1^2}$$

– dynamic inductance;

$$R\approx\frac{\pi(k_1+k_2)}{4k_t^2\omega_1C_0}$$

– dynamic resistance of radiation loss; ω_1 – electrical resonance frequency;

$$\omega_0=\frac{\pi\upsilon^D}{l_0}$$

– mechanical resonance frequency; k_1, k_2 – relative wave impedance (relative to the wave impedance of piezoceramics) of the rear (air) and working loads (acoustic lens made of polystyrene) of the piezoelectric transducer.

The frequencies ω_1 and ω_0 for $R_a=0$ are related by the ratio:

$$\frac{\mathrm{tg}(\pi\omega_1/2\omega_0)}{(\pi\omega_1/2\omega_0)}=\frac{1}{k_t^2}\ \text{or}\ \frac{\omega_1}{\omega_0}\approx\sqrt{1-\frac{8k_t^2}{\pi^2}}.$$

The above circuit (Fig. 8, *a*) is most accurate for $k_1+k_2<<1$, since at a frequency ω_1 it is a parallel connection of capacitance C_0 and equivalent load resistance $R(\omega_1)$ (Fig. 8, *b*), and at a frequency ω_0 – serial connection of the same capacitor C_0 and resistance

$$R_{a0}=\frac{1}{\omega_0C_0}\frac{4k_t^2}{\pi}\frac{1}{k_1+k_2}\approx\frac{1}{\omega_0C_0R}\ \text{(Fig. 8, }c\text{)},$$

i. e., parallel or serial circuits of active and reactive resistances are possible for the entire frequency range $0<\omega<2\omega_0$.

The serial circuit is especially convenient for replacing the piezoelectric element in which ultrasonic waves are received at the mechanical resonance frequency, as in the case of acoustic thermometer.

The parameters of the serial circuit are related to the above measured values U_1, U_2 and φ by the ratios (4). Passing from the circuit (Fig. 8, *a*) to the circuit (Fig. 8, *c*), from (3) we can obtain:

$$R_a=\frac{R_{a0}}{1+\left(Q_a\left(1/x-x\right)\right)^2};$$

$$X_e=\frac{R_{a0}Q_a\left(1/x-x\right)}{1+\left(Q_a\left(1/x-x\right)\right)^2}-\frac{1}{x\omega_0C_0},\tag{4}$$

where

$$x=f/f_0,\ Q_a=\omega_0C_0R_{a0}=\frac{\pi}{2(k_1+k_2)},\ k_1+k_2=\pi/(2Q_a).$$

At the final stage of the research, the temperature dependence of electric noise voltage at the FPT electrodes was obtained (Fig. 9). Water was used as a load, since the acoustic characteristics (specific acoustic impedance) of water and biological objects are identical.

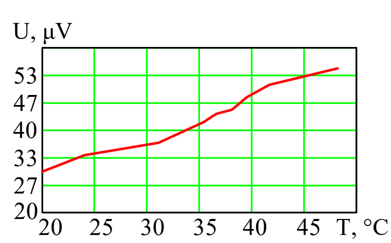

Fig. 9. Experimental temperature dependence of electric noise voltage at the FPT electrodes loaded with water through a polystyrene lens

Processing of the experimental data in accordance with [14] showed that the error of the measurement result for the given confidence level $P = 0.95$ was within $\delta_0 =$ 13 %. The upper and lower boundaries of the confidence interval were compared with the boundaries of the confidence interval calculated in accordance with [14] by the found value of the standard error of the measured voltage.

6. Discussion of the results of the study of the single-channel focussed acoustic thermometer model

The results of laboratory studies confirm the correctness of the model of the single-channel focused AT. Indeed, Fig. 5 shows that the normalized frequency response of the FPT and NS equivalent circuits is substantially the same, and the measured natural noise levels of the circuit (Table 1) correspond to theoretically calculated ones. In turn, it follows that the proposed AT implementing the modified zero modulation method allows measuring noise voltages in the range of 5…30 μV. The latter relates to solving the problem of reducing the level of natural noise of the receiving path by using electronic switching of signals from the output of the noise simulator and the equivalent circuit of the focused piezoelectric transducer. This circuitry solution made it possible to exclude the mechanical modulator unit used in analogs from the acoustic thermometer circuit.

Analysis of the frequency response of the piezoelectric transducer, experimentally obtained by the developed method, based on relations (4), showed that at the mechanical resonance frequency $f_0 = 0.885\,\text{MHz}$, determined by the position of the maximum R_a (Fig. 7, *a*), the reactance

$$X_{c0} = \frac{1}{\omega_0 C_0} = X_e(f_0) = 1{,}628\,\text{Ohm},$$

therefore

$$C_0 = \frac{1}{\omega_0 X_e(f_0)} \approx 1.1 \cdot 10^{-10}\ F.$$

Acoustic Q-factor of the piezoelectric transducer:

$$Q_a \approx \frac{f_0}{\Delta f},$$

where $\Delta f = 0.05\,\text{MHz}$ (the band along the curve $R_a(f)$ is determined by the level of 0.5):

$$R_{a0} = R_a(f_0) = 1{,}411\,\text{Ohm};\quad \frac{R_{a0}}{X_{C_0}} = 0.87;\quad Q_a = 17.7;$$

$$k_1 + k_2 = \frac{\pi}{2Q_a} = 0.089;\quad k_t = 0.23.$$

These results allowed controlling the assembly quality of the focused piezoelectric receiver and confirmed the absence of deviations of the values of the piezoelectric receiver parameters from the theoretical ones.

However, it should be noted that the studies of the temperature dependence of electric noise voltage at the electrodes of the focused piezoelectric receiver, loaded through an acoustic elliptical lens on water, do not take into account the heterogeneity of the structure of real biological tissues. This fact indicates a drawback of the proposed method and necessitates further studies aimed at improving the developed method, taking into account the indicated features of biological objects.

In the future, the results can be used in the development of a model of the focused AT.

7. Conclusions

1. For experimental confirmation of the possibility of deep temperature measurement with a given accuracy, the model of a single-channel passive focussed acoustic thermometer implementing the modified zero modulation method is proposed. The model based on the plate piezoelectric transducer, acoustic elliptical lens and blocks of two serial voltmeters allows measuring noise voltages in the range of 5…30 μV with sufficient simplicity. The determining factor in solving this problem is the use of the original electronic switching unit of the output signals of the noise simulator and the equivalent circuit of the focused piezoelectric transducer.

2. The studies of the temperature dependence of electric noise voltage at the electrodes of the focused piezoelectric receiver, loaded through the acoustic elliptical lens on water, carried out according to the developed method, showed that the total measurement error, taking into account the mean square error 7.9 %, does not exceed 9 %. It should be noted that the proposed method of internal temperature measurement allows getting a measurement accuracy of 0.2 °C, reducing the measurement time to ~1 s and measuring temperature in the dynamic mode. Spatial resolution of ~1 mm at a depth of 10 cm is much better than with an elliptical mirror radiothermograph.

References

1. Naida, S. A. (2002). Acoustothermometry of liquid objects using priezoelectronic receivers of megahertz range. Tehnicheskaya diagnostika i nerazrushayushchiy kontrol', 3, 41–48.
2. Bowen, T. (1987). Acoustic radiation temperature for noninvasive thermometry. Automedica (UK), 8 (4), 247–267.
3. Anosov, A. A., Kazansky, A. S., Subochev, P. V., Mansfel'd, A. D., Klinshov, V. V. (2015). Passive estimation of internal temperatures making use of broadband ultrasound radiated by the body. The Journal of the Acoustical Society of America, 137 (4), 1667–1674. doi: https://doi.org/10.1121/1.4915483
4. Anosov, A. A., Sharakshane, A. A., Kazanskii, A. S., Mansfel'd, A. D., Sanin, A. G., Sharakshane, A. S. (2016). Instrument function of a broadband acoustic thermometric detector. Acoustical Physics, 62 (5), 626–632. doi: https://doi.org/10.1134/s1063771016050018
5. Anosov, A. A., Belyaev, R. V., Klin'shov, V. V., Mansfel'd, A. D., Subochev, P. V. (2016). Passive broadband acoustic thermometry. Technical Physics, 61 (4), 597–602. doi: https://doi.org/10.1134/s1063784216040058

6. Anosov, A. A., Subochev, P. V., Mansfeld, A. D., Sharakshane, A. A. (2018). Physical and computer-based modeling in internal temperature reconstruction by the method of passive acoustic thermometry. Ultrasonics, 82, 336–344. doi: https://doi.org/10.1016/j.ultras.2017.09.015
7. Drozdenko, E. S., Naida, S. A. (2009). O vliyanii detektirovaniya shuma na tochnost' izmereniya temperatury akustotermometrom. Elektronika i svyaz', 6, 62–67.
8. Naida, S. A., Drozdenko, K. S. (2012). The modified scheme of deep temperature measurement zero modulation method. Systemy obrobky informatsiyi, 5, 47–52.
9. Drozdenko, K. S. (2013). Single-channel focusable acoustothermometer for measuring the internal temperature of biological object. Radioelectronics and Communications Systems, 56 (4), 207–211. doi: https://doi.org/10.3103/s0735272713040067
10. Agarwal, A., Lang, J. (2005). Foundations of Analog and Digital Electronic Circuits. Morgan Kaufmann Publishers is an imprint of Elsevier, 1008.
11. Bakshi, U. A., Godse, A. P. (2009). Analog And Digital Electronics. Technical Publications, 547.
12. Kino, G. S. (1987). Acoustic waves: Devices, imaging, and analog signal processing. Prentice Hall, 601.
13. Beranek, L. L., Mellow, T. J. (2012). Acoustics: Sound Fields and Transducers. Academic Press, 720.
14. Preobrazovateli, antenny gidroakusticheskie. Metodiki izmereniya parametrov na ispytatel'nyh bazah predpriyatiya: RD 5.0542-86 (1990). Kyiv: Minsudprom.